Optimisation de forme de structures élancées viscoélastiques, application et analyse

Antoni Joubert, Grégoire Allaire, Samuel Amstutz, Julie Diani

Homogeneization in (reinforced) Polymers

Mean-field approach

Semi-crystalline polymers

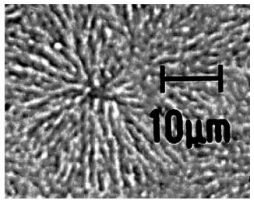

$$\mathbf{C}^{c}_{PP} = \begin{pmatrix} 7.78 & 3.91 & 3.72 & 0 & 0.9 & 0 \\ 3.91 & 11.55 & 3.99 & 0 & -0.36 & 0 \\ 3.72 & 3.99 & 42.44 & 0 & -0.57 & 0 \\ 0 & 0 & 0 & 4.02 & 0 & -0.12 \\ 0.9 & -0.36 & -0.57 & 0 & 3.1 & 0 \\ 0 & 0 & 0 & -0.12 & 0 & 2.99 \end{pmatrix} \text{GPa}$$

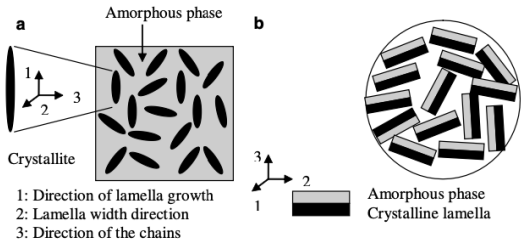

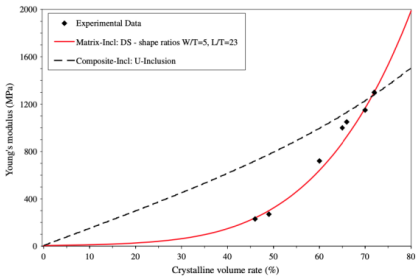

Crystalline lamellae shape factor PP vs. PE

F. Bédoui, G. Régnier (2004-2006)

Carbon-black reinforced elastomers

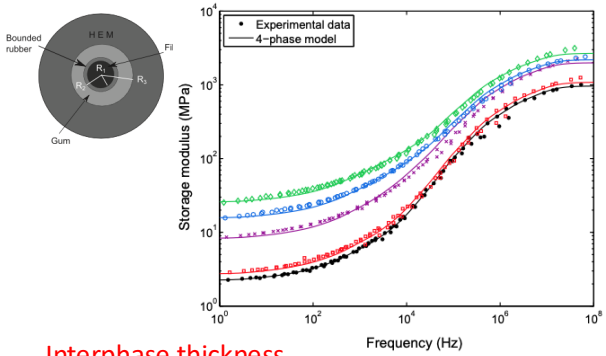

Interphase thickness
Interphase viscoelastic behavior

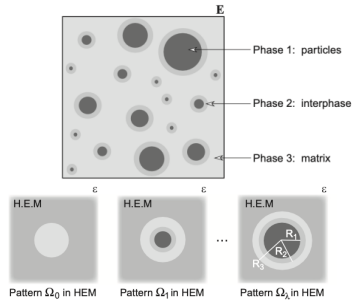

Particle size distribution
Particle interdistance distribution

P. Gilormini, Y. Merckel, F. Vion-Loisel (2013,2014)

Full-field

Propellants

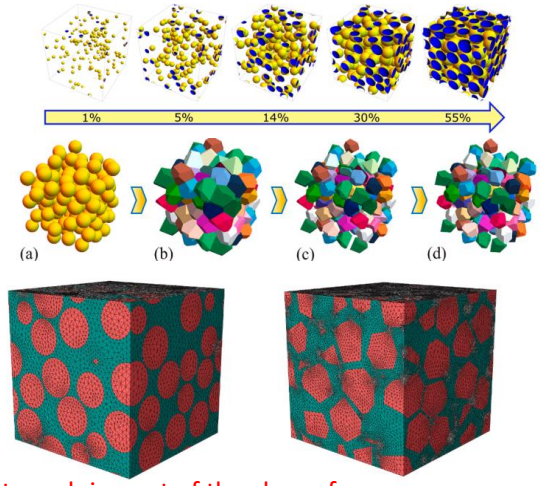

Not much impact of the shape for similar shape factors

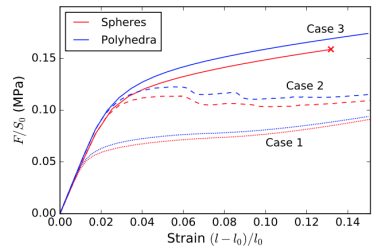

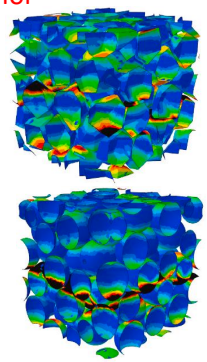

F. de Francqueville, P. Gilormini (2019-2021)

Material_Homogeneization_Jupyter_notebook

Homogeneization in (reinforced) Polymers

Full-field approach

Soft matrix with high volume fraction of particles or voids

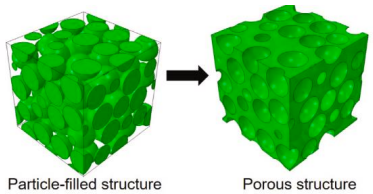

Neo-Hookean matrix
55% particles/voids

Remeshing
Analytical solutions

Particles

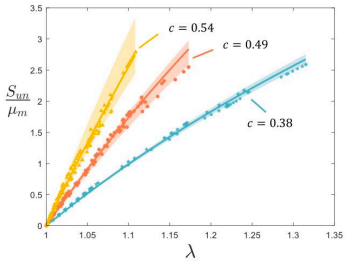

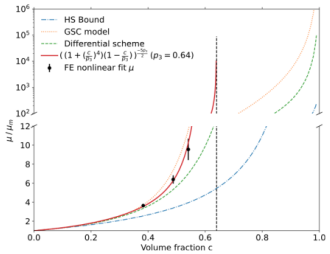

Pores

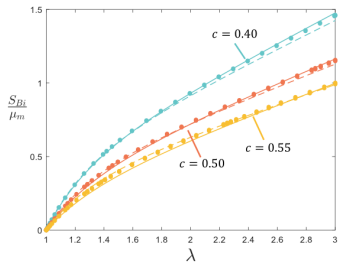

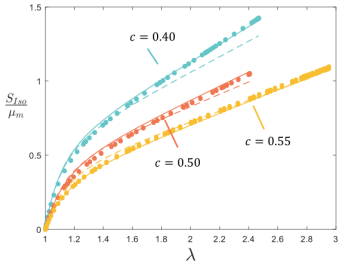

H. Luo, Z. Hooshmand-Ahoor, K. Danas (2023)

Viscoelastic behavior of Interpenetrated polymer network

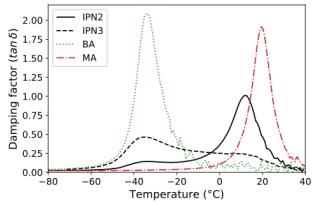

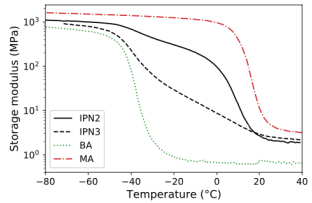

Homogeneization by FFT method

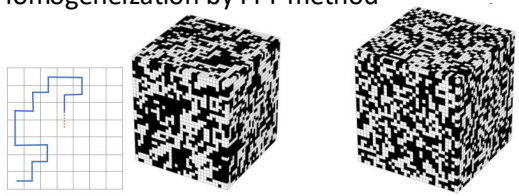

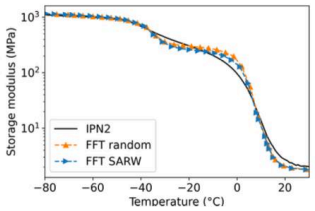

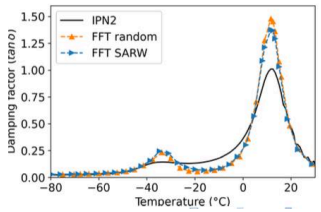

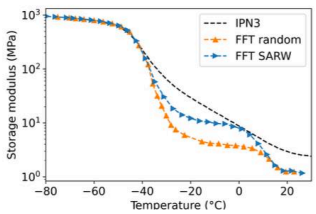

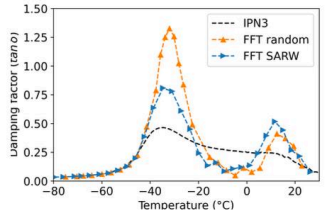

(2021)

Viscoelasticity of anisotropic carbon fibers reinforced thermoplastics

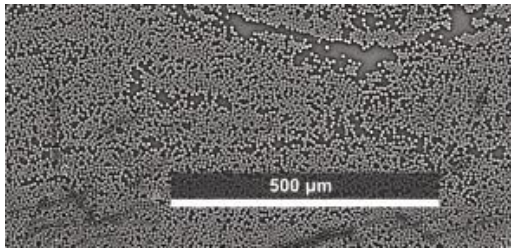

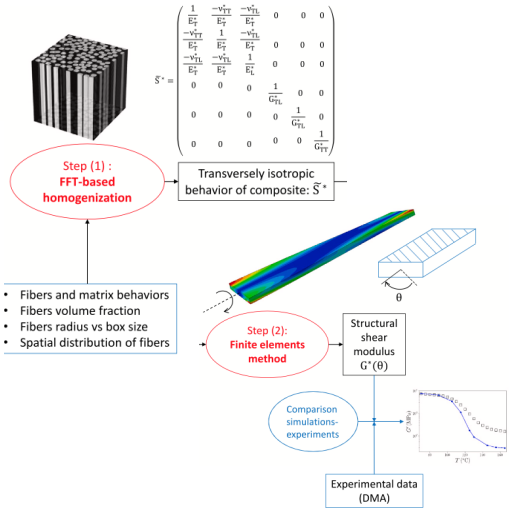

T. Merlette (2025)

Optimisation de forme de structures élancées viscoélastiques, application et analyse

Antoni Joubert, Grégoire Allaire, Samuel Amstutz, Julie Diani

Objective

[Arkema]

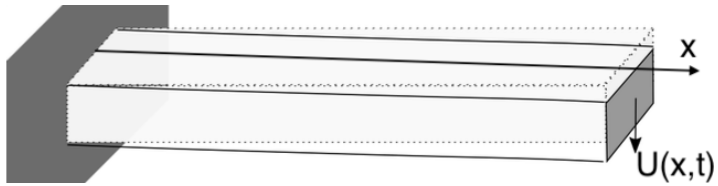

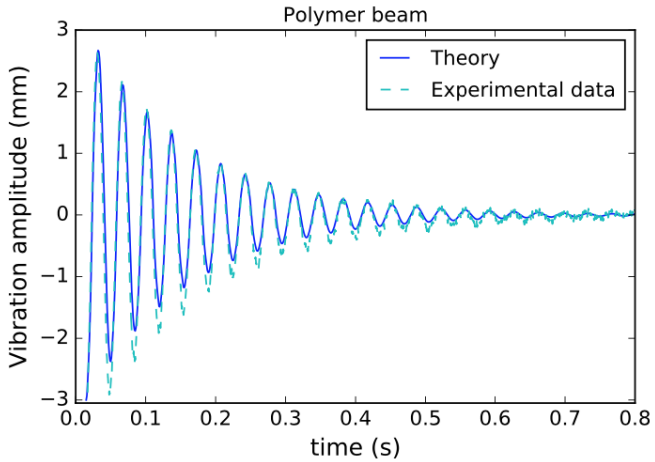

Euler-Bernouilli beam $\sigma(t) = \int_{-\infty}^{t} E(t-\tau)\dot{\epsilon}(\tau)d\tau$

$E(t) = E_\infty + \sum_{j=0}^{n} E_j e^{-t/\tau_j}$, $U(x,t) = u(x)e^{i\omega t}$,

$\omega = \omega_r + i\omega_i$

Euler-Bernouilli cantilever beam under free vibration

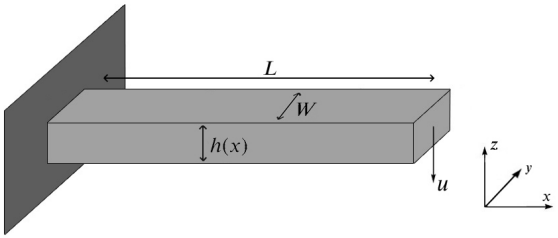

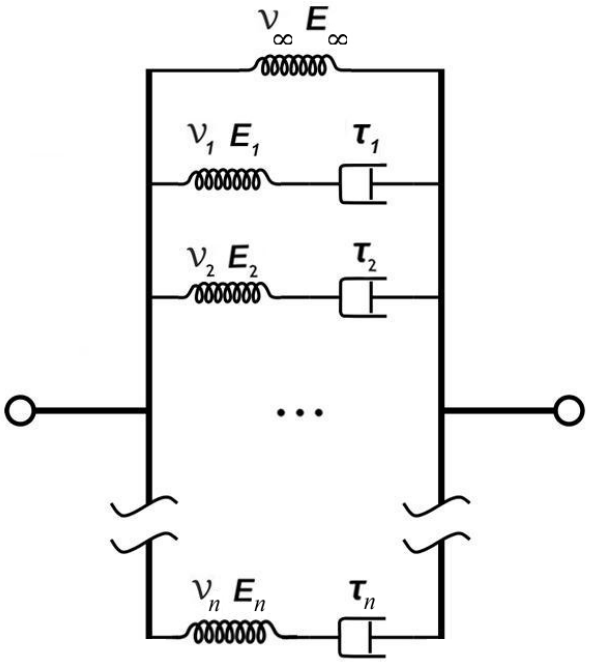

$$\int_{\Omega^{3D}} \rho \frac{\partial^2 U}{\partial t^2} \hat{u} dV + \int_{\Omega^{3D}} \sigma.\epsilon(\hat{u}) dV = 0, \forall t \in \mathbb{R}_+$$

Linear viscoelastic behavior

$$\sigma(M,t) = E_\infty \epsilon(U)(M,t) + \sum_{j=1}^{n} E_j \int_{-\infty}^{t} e^{-\frac{t-\tau}{\tau_j}} \frac{\partial \epsilon(U)}{\partial \tau}(M,\tau) d\tau$$

Bending strain

$$\epsilon(U)(x,y,z,t) = -z \frac{\partial^2 U}{\partial x^2}(x,t), \quad U(x,t) = u(x) e^{i\omega t}$$

Problem to solve

$$\int_0^L \frac{h^3}{12\rho} \frac{d^2 u}{dx^2} \frac{d^2 \hat{u}}{dx^2} dx = \frac{\omega^2}{E_\infty + \sum_{j=1}^{n} E_j \frac{i\omega\tau_j}{1+i\omega\tau_j}} \int_0^L h u \hat{u}\, dx, \forall \hat{u} \in \mathcal{U}_0$$

$a(h,u,\hat{u}) = \lambda(h) b(h,u,\hat{u})$ with $\lambda \in \mathbb{R}$

Objective function

- Maximizing or limiting the damping
- First mode of vibration $\omega = \omega_r + i\,\omega_i$
- Logarithmic decrement $\dfrac{\omega_i}{\omega_r}$, Decay rate of the vibration ω_i
- Minimize $\mathcal{J}(\lambda) = -\frac{\omega_i(\lambda)}{\omega_r(\lambda)} = j(h)$
- Gradient method, sensitivity analysis with respect to h
  Derive $a(h,u,\hat{u}) = \lambda(h) b(h,u,\hat{u})$ with $\lambda \in \mathbb{R}$

$$D_h a(h,u,\hat{u})\tilde{h} + a(h, D_h u\tilde{h}, \hat{u}) =$$
$$D\lambda(h)\tilde{h} b(h,u,\hat{u}) + \lambda(h)\left(D_h b(h,u,\hat{u})\tilde{h} + b(h, D_h u\tilde{h}, \hat{u})\right) \quad \forall \hat{u} \in \mathcal{W}_0.$$

$$Dj(h)\tilde{h} =$$
$$-\frac{\omega_r(\lambda(h))\frac{\partial \omega_i}{\partial \lambda}(\lambda(h)) - \omega_i(\lambda(h))\frac{\partial \omega_r}{\partial \lambda}(\lambda(h))}{\omega_r^2(\lambda(h))} \int_0^L \left(\frac{1}{4\rho} h^2 \frac{\left(\frac{d^2 u}{dx_1^2}\right)^2}{\int_0^L h u^2 dx_1} - \lambda(h) \frac{u^2}{\int_0^L h u^2 dx_1} \right) \tilde{h}\, dx_1$$

Numerical resolution

- Bending problem of the 4th order $\rightarrow$ mixed formulation $v = -\frac{h^3}{12\rho}\frac{d^2u}{dx_1^2}$
- Suite minimisante $h_{k+1} = h_k - t_k d_k$, $d_k = \frac{j'(h_k)}{||j'(h_k)||}$
- Gradient is regularized using H^1 inner product,

$$\langle j'(h), \tilde{h} \rangle_{H^1} = \int_0^L \left(\eta^2 \frac{dj'(h)}{dx}\frac{d\tilde{h}}{dx} + j'(h)\tilde{h} \right) dx$$

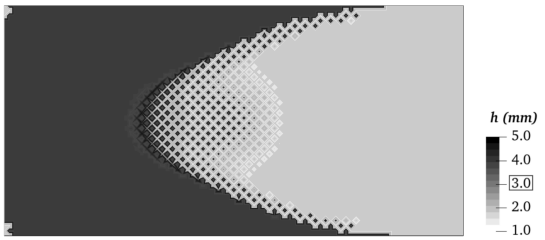

- Thickness bounds $[h_{min}, h_{max}]$ and volume $V(h) = \int_0^L h(x)dx = V_0$ constraints satisfied by projection
  $\Big(P_{ad}(h)\Big)(x_1) = max\left(h_{min}, min(h_{max}, h(x_1) + \ell)\right)$
  ℓ is dettermined by bisection such as $\int_0^L P_{ad}(h)dx_1 = V_0$
- FreeFem++, P1 elements, ARPACK library
- Algorithm stop criterion relative change of cost function, iteration number
- Initial beam LxT = 60x3 mm^2

Viscoelastic behavior

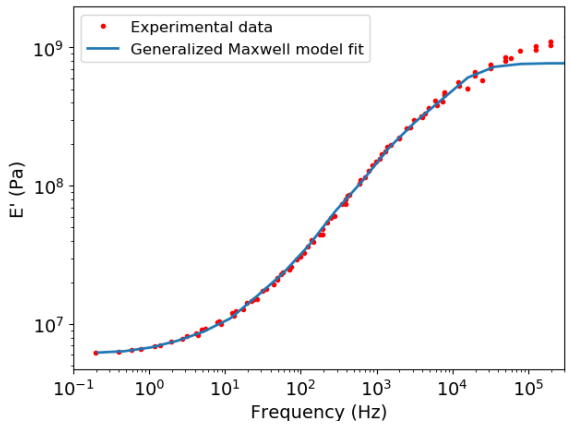

Cost function evolution

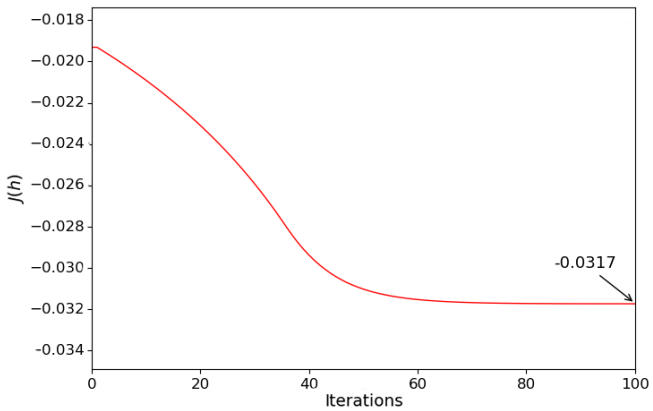

Optimize profile for optimized damping

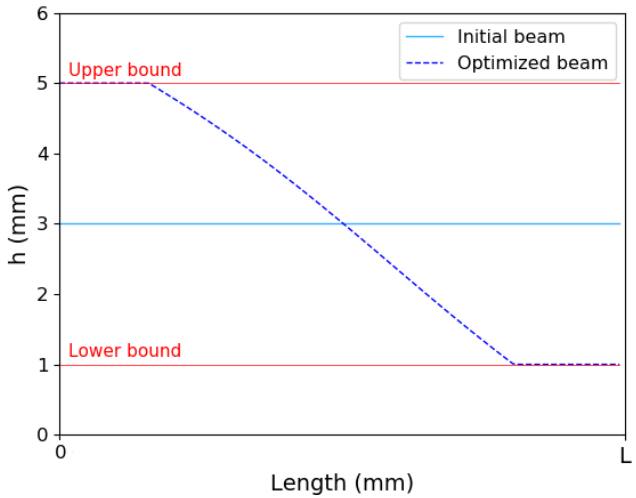

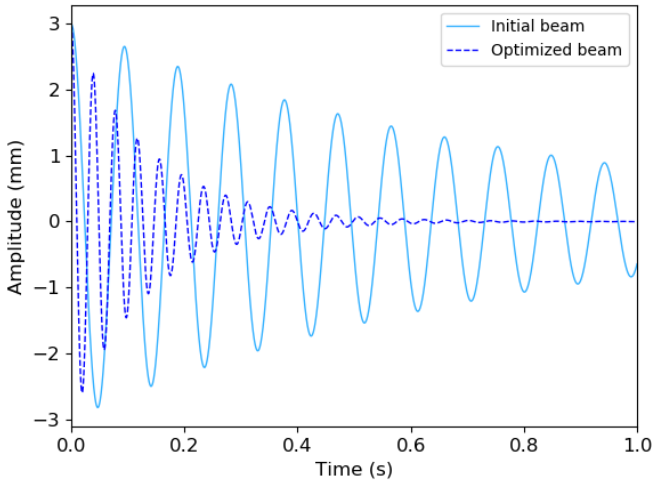

Free vibration of cantilever plates

- Kirchhoff-Love plates

Plane strain tensor

$$\epsilon(U)(x,y,z,t) = \begin{pmatrix} \epsilon_1 \\ \epsilon_2 \\ \gamma_{12} \end{pmatrix} = \begin{pmatrix} -z\frac{\partial^2 U}{\partial x^2} \\ -z\frac{\partial^2 U}{\partial y^2} \\ -2z\frac{\partial^2 U}{\partial x \partial y} \end{pmatrix}$$

Bending plane stress tensor

$$\sigma(x,y,z,t) = C_\infty \epsilon(U)(x,y,z,t) + \int_{-\infty}^{t} R(t-\tau)\frac{\partial \epsilon(U)}{\partial \tau}(x,y,z,\tau)d\tau,$$

with

$$C_\infty = \begin{pmatrix} \frac{E_\infty}{1-\nu_\infty^2} & \nu_\infty \frac{E_\infty}{1-\nu_\infty^2} & 0 \\ \nu_\infty \frac{E_\infty}{1-\nu_\infty^2} & \frac{E_\infty}{1-\nu_\infty^2} & 0 \\ 0 & 0 & \frac{E_\infty}{2(1+\nu_\infty)} \end{pmatrix} \quad R(\tau) = \sum_{j=1}^{n} \begin{pmatrix} \frac{E_j}{1-\nu_j^2} & \nu_j \frac{E_j}{1-\nu_j^2} & 0 \\ \nu_j \frac{E_j}{1-\nu_j^2} & \frac{E_j}{1-\nu_j^2} & 0 \\ 0 & 0 & \frac{E_j}{2(1+\nu_j)} \end{pmatrix} e^{-\frac{\tau}{\tau_j}}$$

- Problem to solve

$$\mathcal{U}_2 = \left\{ u \in H^2(\Omega, \mathbb{C}) \mid u_{|\Gamma_D} = 0, \frac{du}{dn}_{|\Gamma_D} = 0 \right\}$$

$$-\omega^2 \rho h \int_\Omega u\hat{u}\, dA + \frac{h^3}{12} \int_\Omega \left((c_{11} - \tilde{r}_{11}) \left(\frac{\partial^2 u}{\partial x^2} \frac{\partial^2 \hat{u}}{\partial x^2} + \frac{\partial^2 u}{\partial y^2} \frac{\partial^2 \hat{u}}{\partial y^2} \right) \right.$$

$$\left. + (c_{12} - \tilde{r}_{12}) \left(\frac{\partial^2 u}{\partial x^2} \frac{\partial^2 \hat{u}}{\partial y^2} + \frac{\partial^2 u}{\partial y^2} \frac{\partial^2 \hat{u}}{\partial x^2} \right) + 2 (c_{33} - \tilde{r}_{33}) \frac{\partial^2 u}{\partial x \partial y} \frac{\partial^2 \hat{u}}{\partial x \partial y} \right) dA = 0.$$

with $c_{kl}(E_\infty, \nu_\infty, E_j, \nu_j)$ and $\tilde{r}_{kl}(E_j, \nu_j, \tau_j, \omega)$ for $kl \in \{11, 22, 12, 33\}$

$\Leftrightarrow$ Complex polynomial eigenproblem of form

$$\sum_{j=0}^{n+2} \omega^j a_j(h, u, \hat{u}) = 0 \qquad \forall \hat{u} \in \mathcal{U}_2,$$

- Mechanical behavior: Constant K or ν? $K = 3$ GPa and $\nu_j = \frac{3K - E_j}{6K}$

Shape and thickness optimization for plates

- Shape optimization by shape derivative

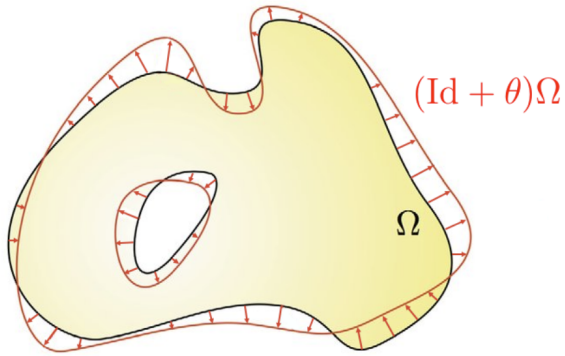

$\Omega_\theta = (Id + \theta)\Omega$ with $\theta \in W^{1,\infty}(\mathbb{R}^2, \mathbb{R}^2)$
Shape derivative of a functional $F(\Omega_\theta)|_\Omega$
$F((Id + \theta)\Omega) = F(\Omega) + D_\Omega F(\Omega)\theta + o(\theta)$ with $\lim_{\theta \to 0} \frac{|o(\theta)|}{\|\theta\|_{W^{1,\infty}}} = 0$

Lemma

Given $f \in W^{1,1}(\mathbb{R}^2)/F(\Omega) = \int_\Omega f(x)dA$, the shape derivative of F

$$D_\Omega F(\Omega)\theta = \int_\Omega \mathrm{div}\big(\theta(x)f(x)\big)dA = \int_{\partial\Omega} f(s)\theta(s).n(s)ds.$$

- Plate bending problem is of fourth order: non-conforming Morley elements

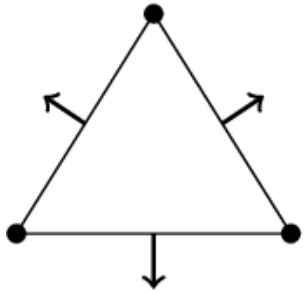

- complex polynomial eigenproblem: SLEPc library
- Alternate thickness (updated at every iteration) and shape optimization (updated every 3 iteration)
- θ updated thanks to the shape derivative of the cost function
- Mesh deformed by the advection field θ and remeshing performed at each update
- θ not only defined on the frontier
- Local minimum, several initializations (LxWxT = 60x30x3 mm^3)

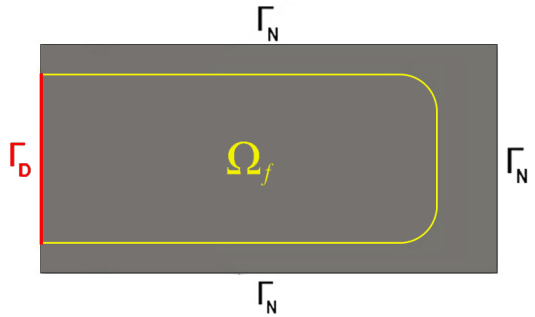

Sizing optimization

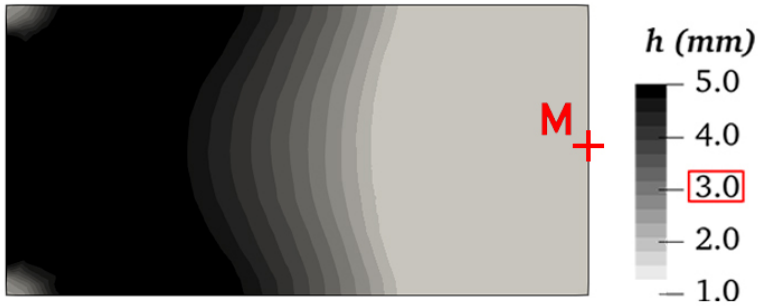

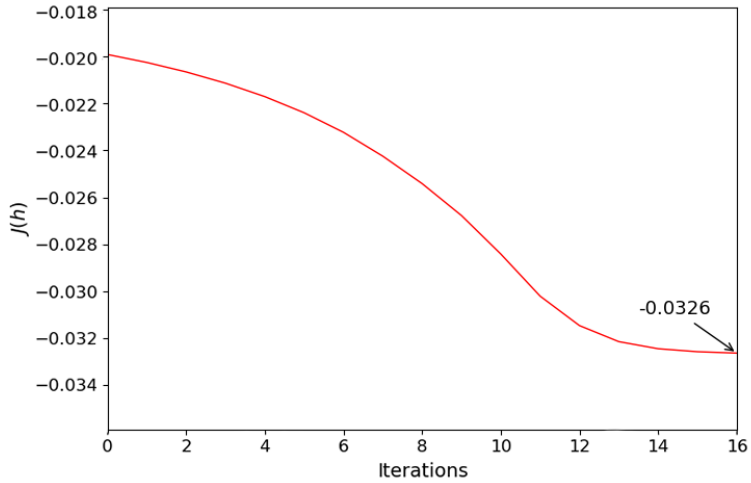

Shape optimization

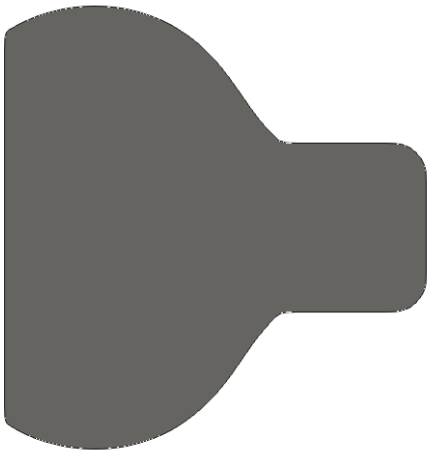

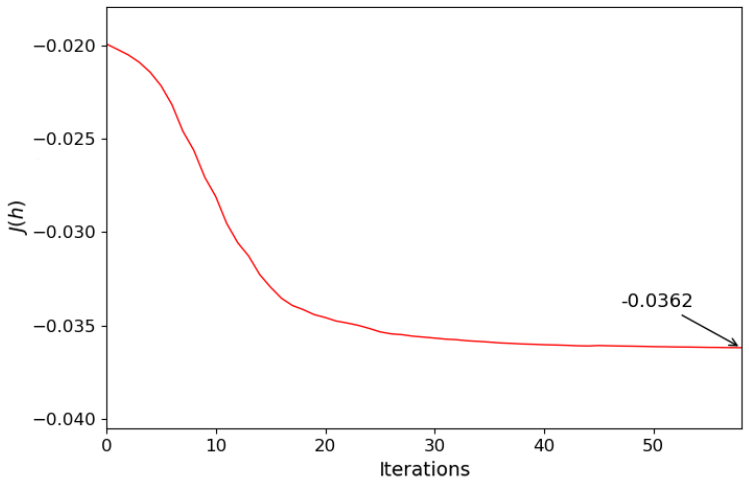

Sizing optimization

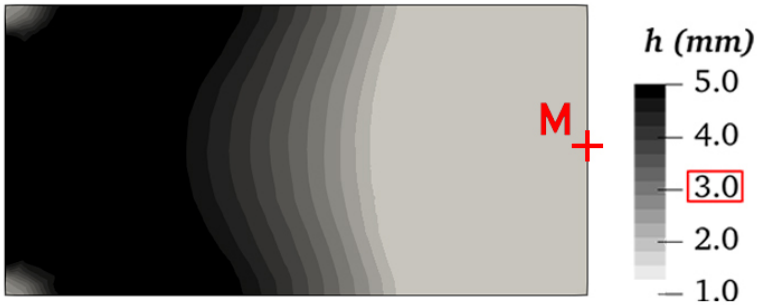

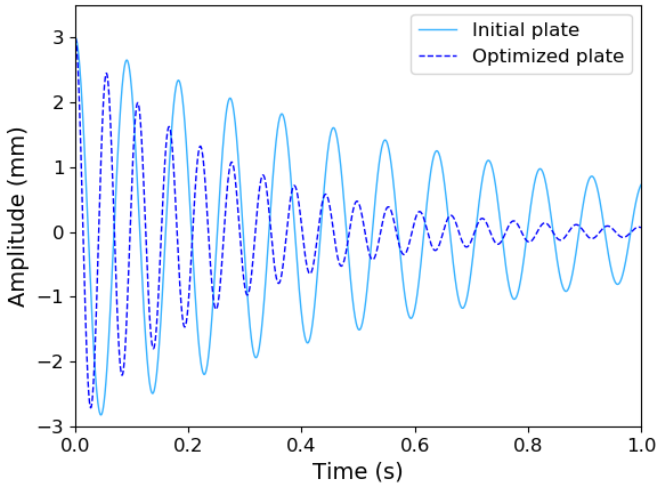

Shape optimization

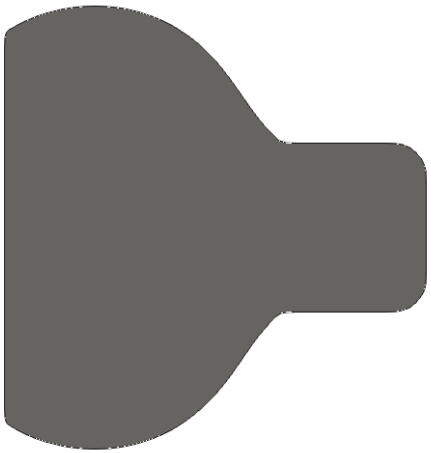

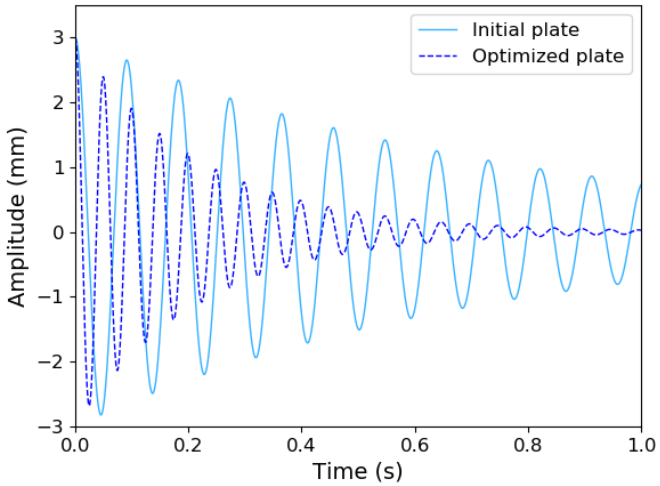

Coupled optimization

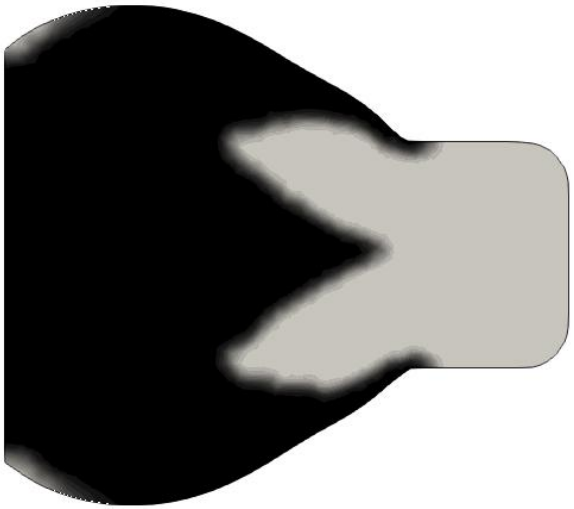

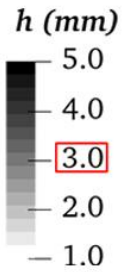

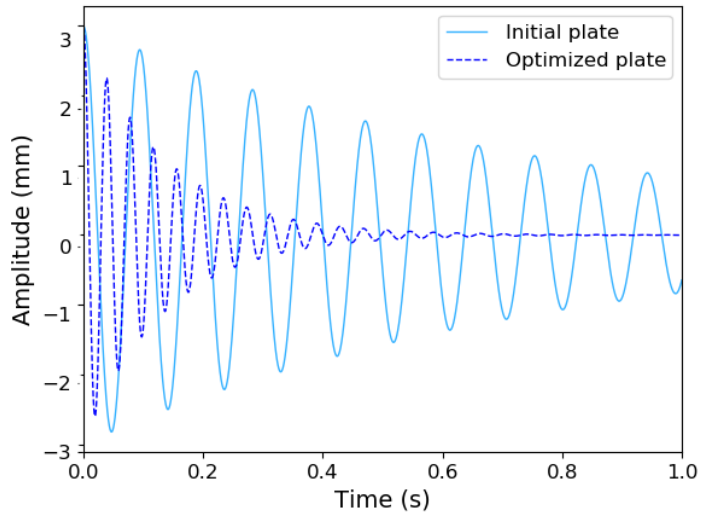

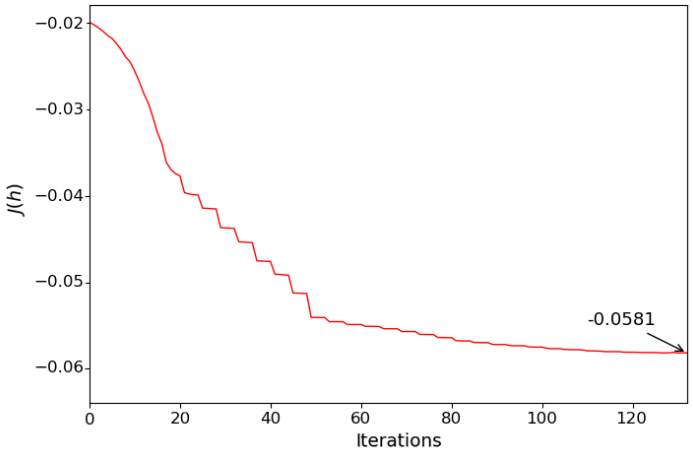

Impact of material parameters: Zener model
Reference: $E_\infty = 18$ MPa, $\nu_\infty = 0.4999$,
$E_1 = 30$ MPa, $\nu_1 = 0.498$, $\tau_1 = 0.002$s

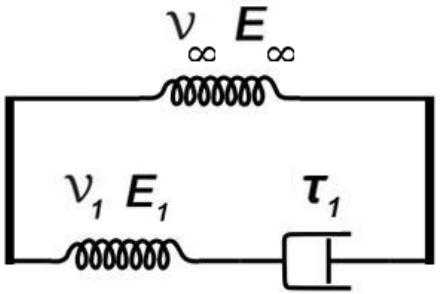

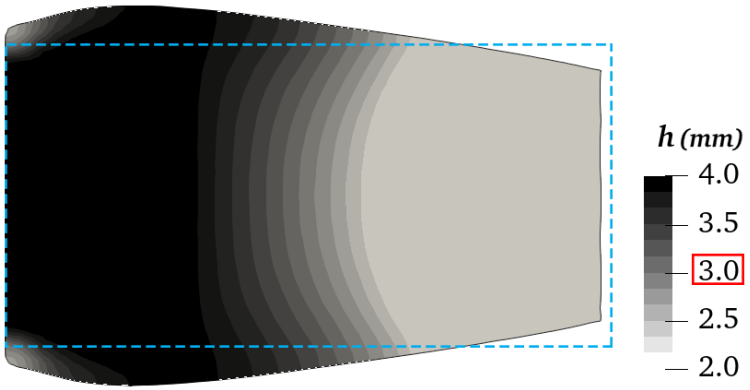

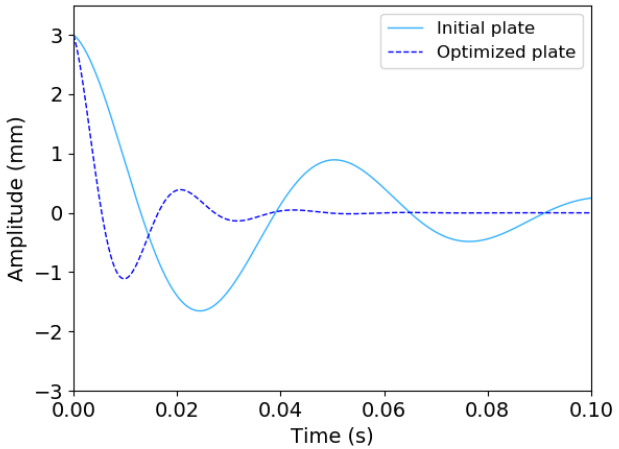

Impact of the Young modulus ratio

$E_1 = 10$ MPa

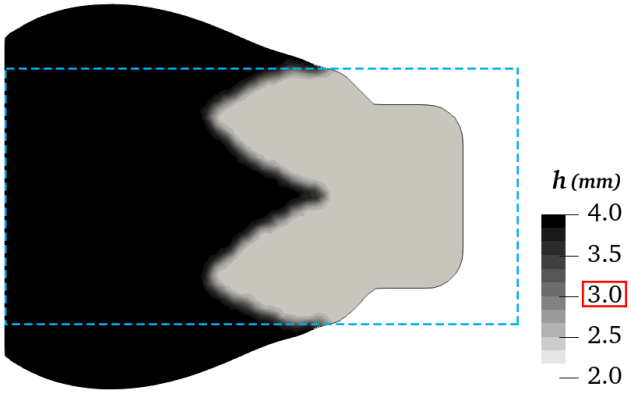

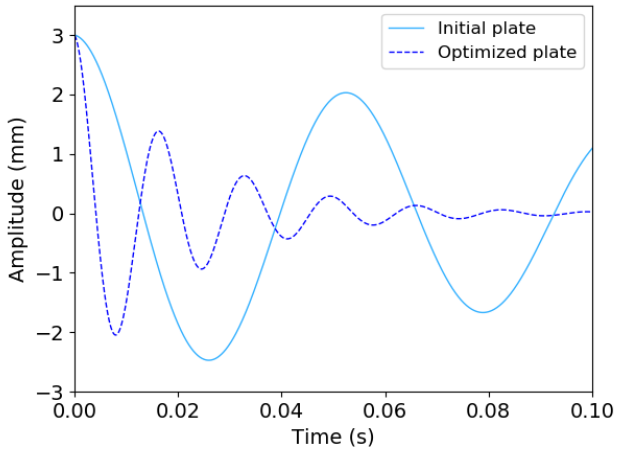

$E_1 = 40$ MPa

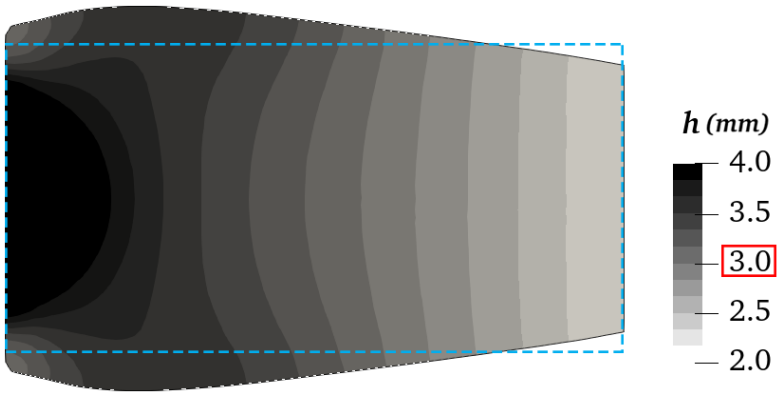

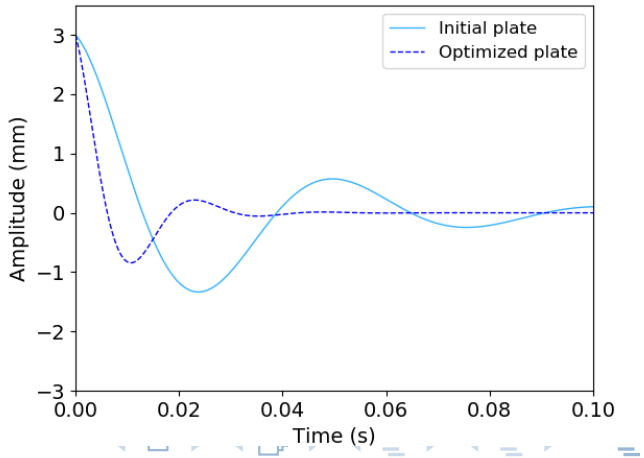

Impact of the relaxation time

$\tau_1 = 0.0005$

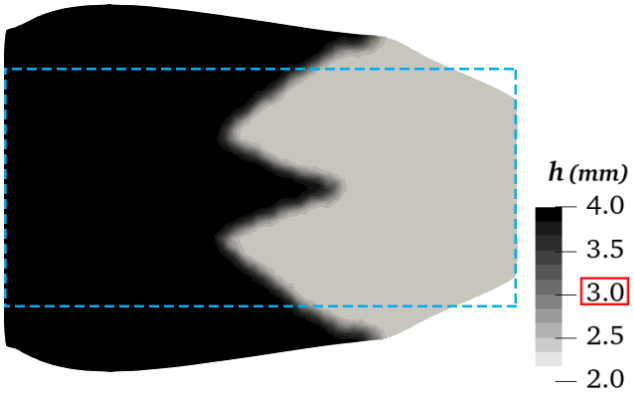

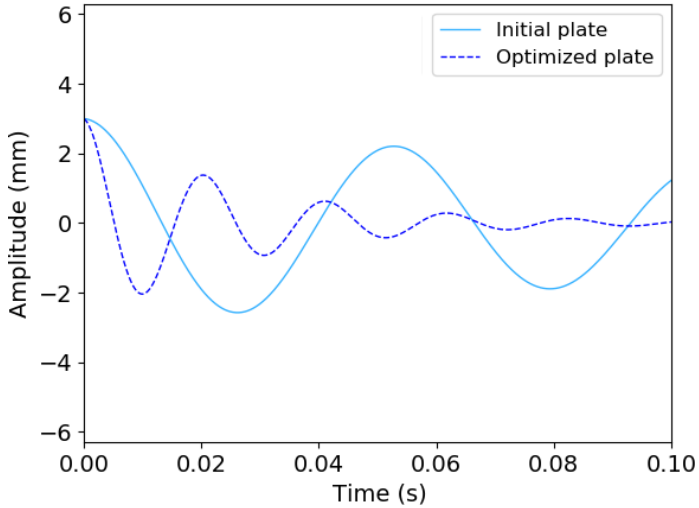

$\tau_1 = 0.005$

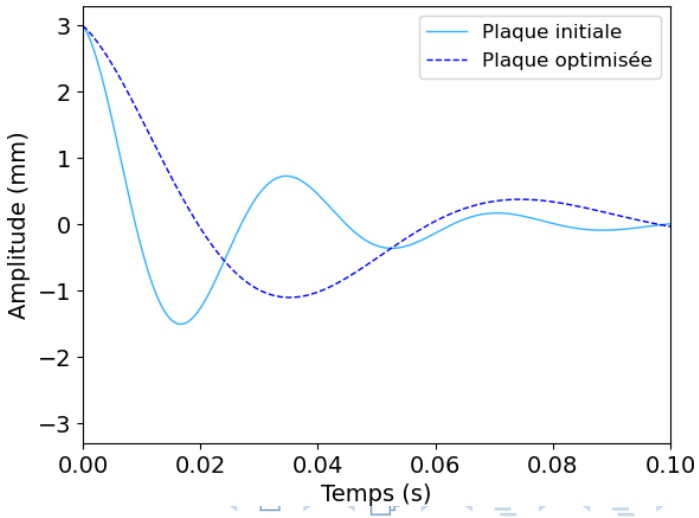

Impact of the Poisson's ratio

$\nu_1 = 0.498$

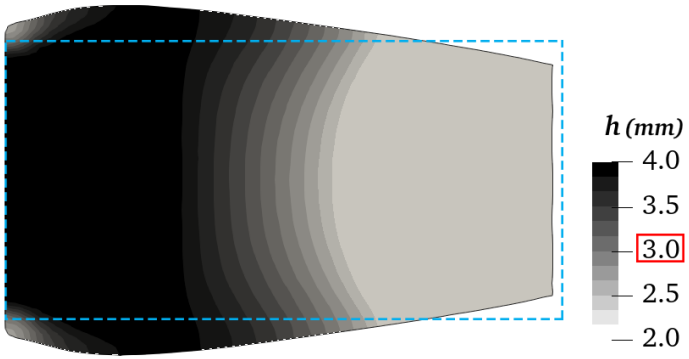

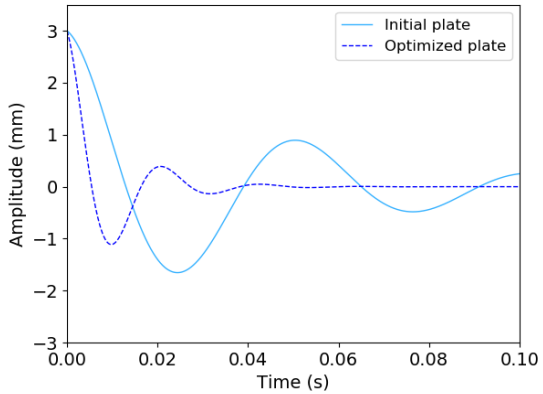

$\nu_1 = 0.4$

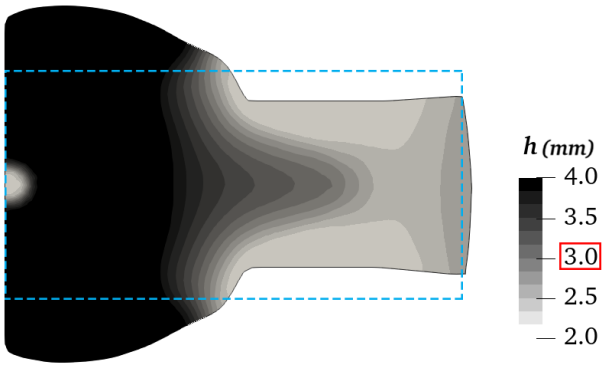

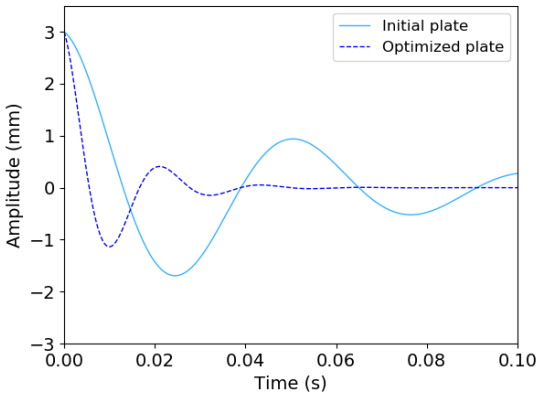

Several designs resulting in similar behaviors: Interesting to accomodate engineering constraints

Generalized Maxwell model with ν constant

According to the other parameters(E_j, τ_j), two cases are possible:

- Sharp thickness transtion

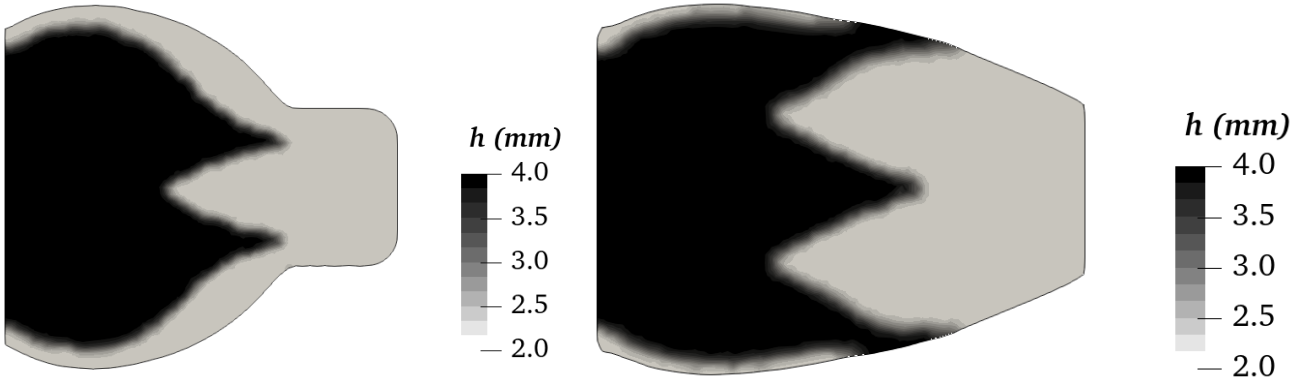

Two designs according to $\nu \leq 0.465$ or $\nu > 0.465$

- Gradual thickness transition

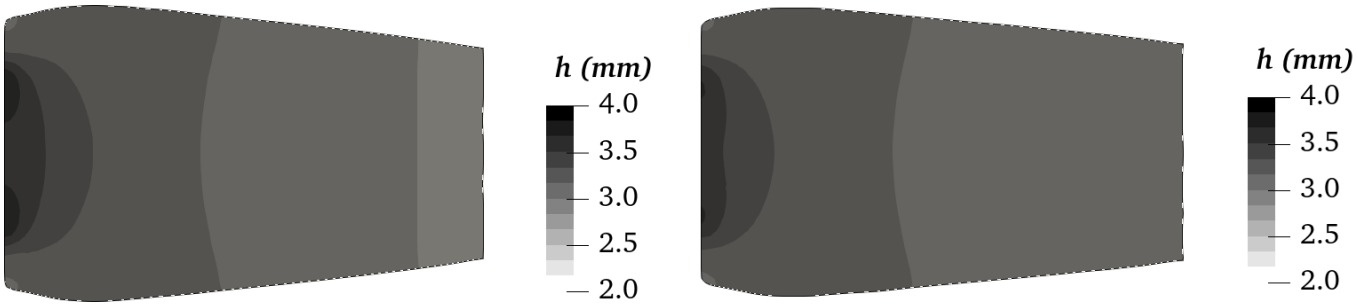

$\nu = 0.2$ $\nu = 0.4$

the design depends on ν but hardly the vibration damping

Optimizing decay rate vs. frequency of vibration

Limiting the damping $\mathcal{J}(h,\Omega) = \omega_i(h,\Omega) + k\frac{1}{\omega_r(h,\Omega)}$

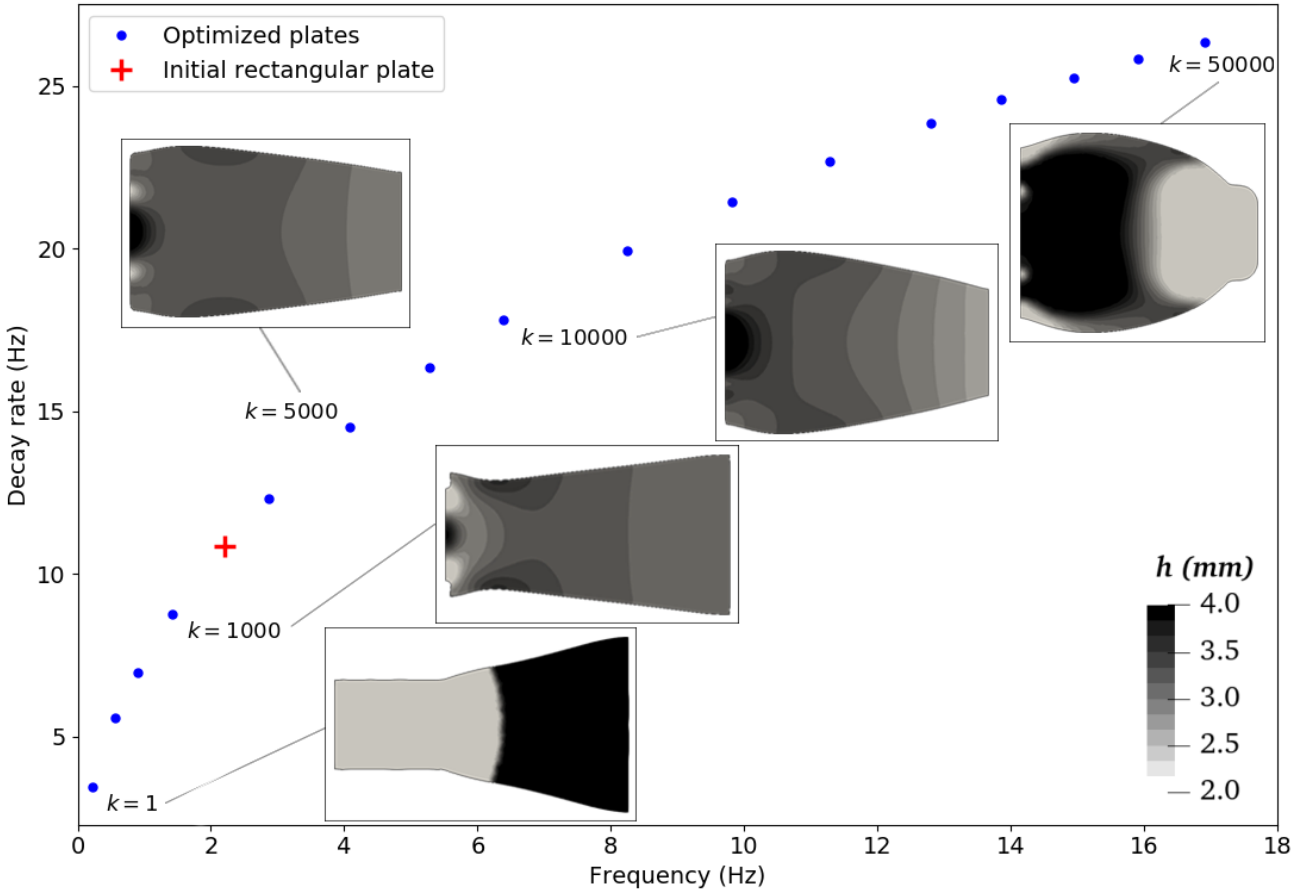

Topology optimization of a running shoe sole

- Vibration test and Bennewart bending

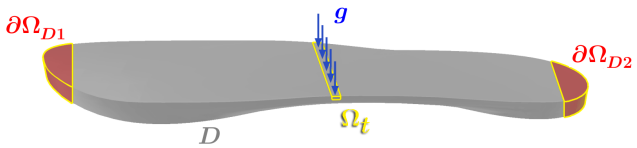

Compliance $C = \int_g g u_g dx$

- Plate problem

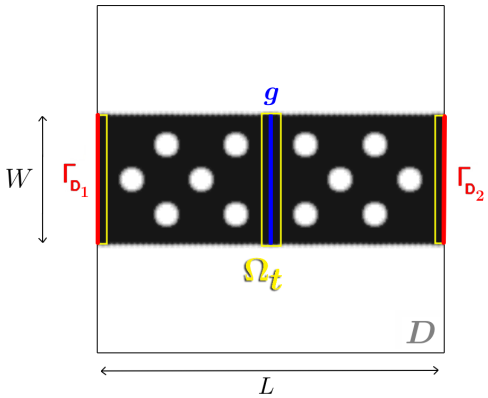

Optimize damping within volume and compliance constraint

$inf_{\Omega \in \mathcal{V}_{ad}} \mathcal{J}(\Omega)$ such that $C(\Omega) \leq C_l$

Increase the bending stiffness of 15%: $C_l = 0.85\, C_0$

Topology optimization

- Optimization problem

$$\inf_{\Omega \in \mathcal{V}_{ad}} \sup_{\substack{\mu_1 \geq 0 \\ \mu_2 \geq 0}} \mathcal{L}(\Omega, \mu),$$

$$\begin{aligned}\mathcal{L}(\Omega, \mu_1, \mu_2) = &- \frac{\omega_i^{D1}(\Omega)}{\omega_r^{D1}(\Omega)} - \frac{\omega_i^{D2}(\Omega)}{\omega_r^{D2}(\Omega)} \\ &+ \frac{1}{2c_1}\left(\left(P_{\mathcal{R}_+}(\mu_1 + c_1(C(\Omega) - C_l))\right)^2 - \mu_1^2\right) \\ &+ \mu_2(V(\Omega) - V_l) + \frac{c_2}{2}(V(\Omega) - V_l)^2\end{aligned}$$

- Level-set method

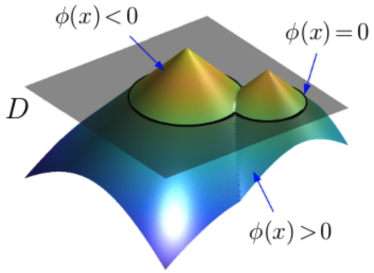

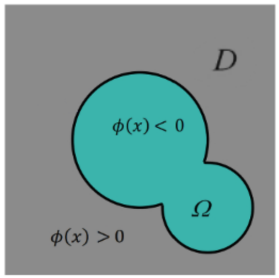

$\frac{\partial \phi}{\partial t} + v(t,x)|\nabla \phi| = 0$ with $v = b(\Omega)$ and $D_\Omega \mathcal{J}(\Omega)(\theta) = \int_\Omega b(\Omega)\theta.n ds$

Topology optimization

Kirchhoff-Love plate submitted to free vibration

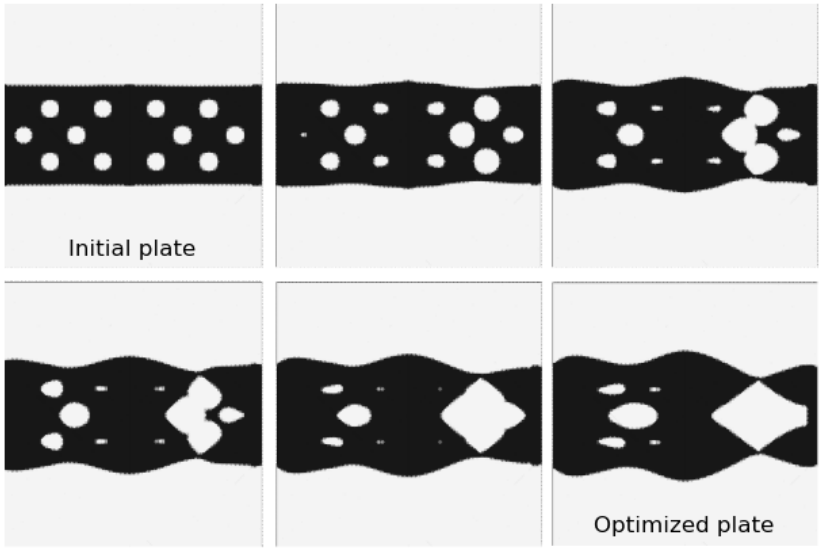

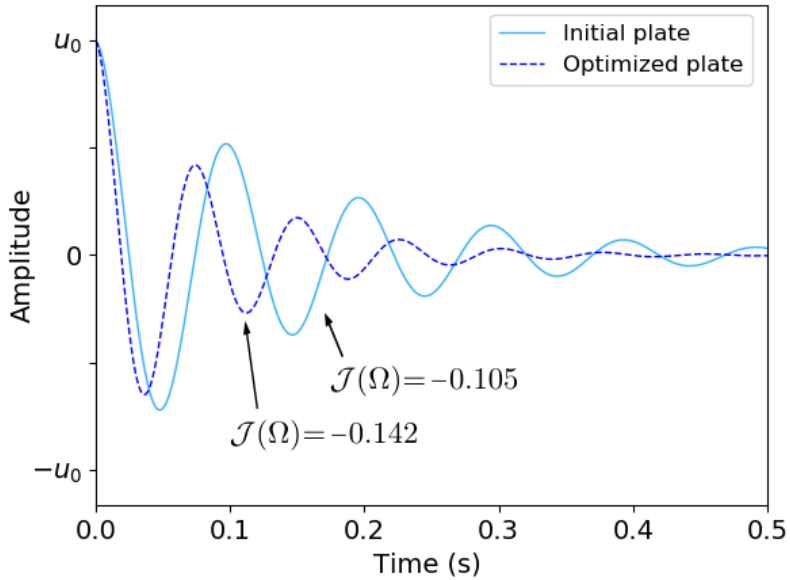

$\Rightarrow$ weak locations in the design

Kirchhoff-Love vs. Reissner-Mindlin

Elastic bending compliance problem

Initial design

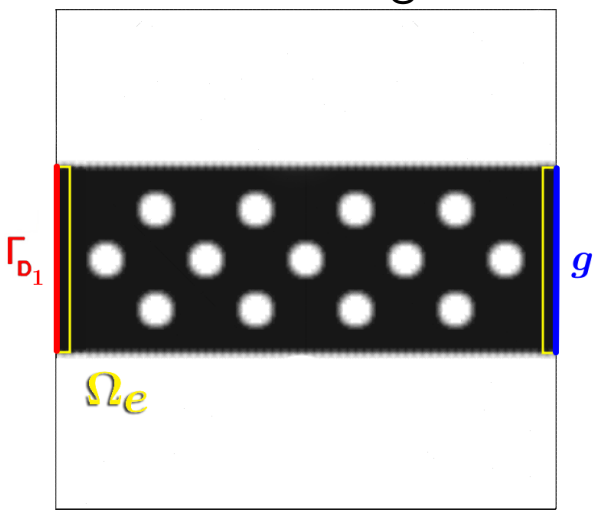

KL design

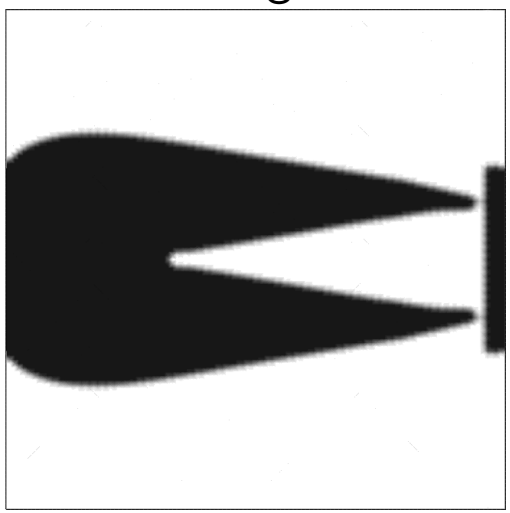

RM design

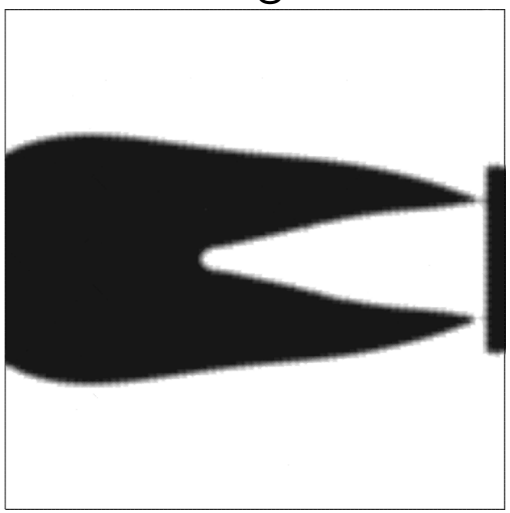

Weak points remain $\Rightarrow$ use of 3D model

Optimal design for 3D bending plate

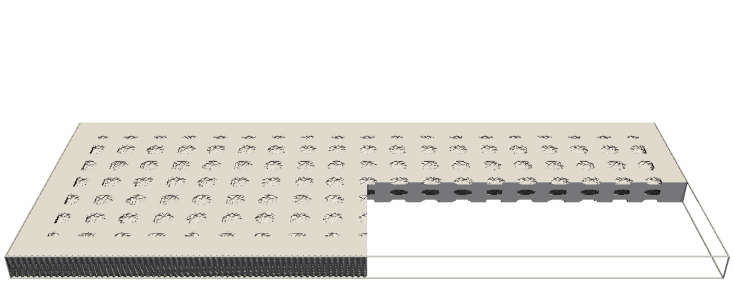
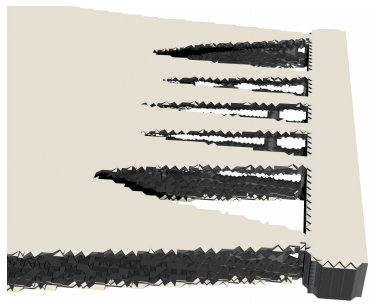
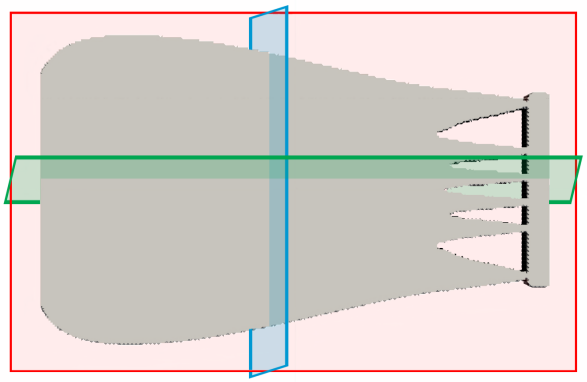
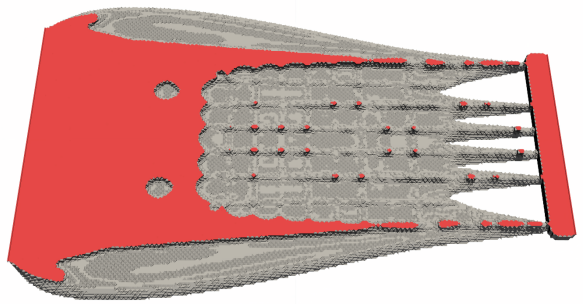

Free vibration of the cantilever 3D plate

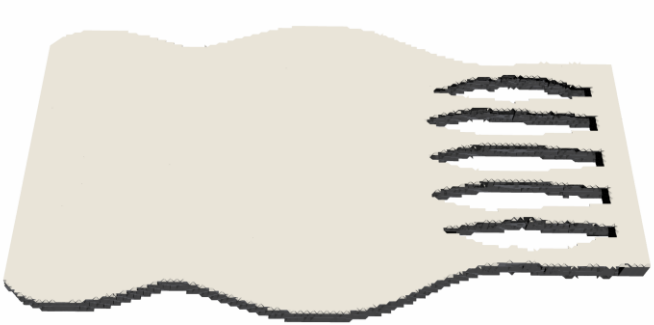

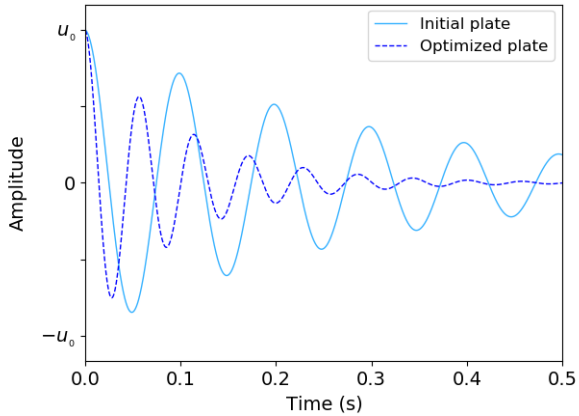

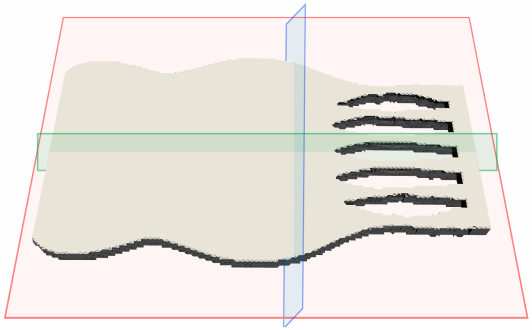

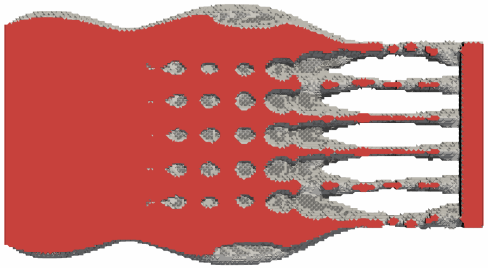

Free vibration of the 3D plate clamped at both end

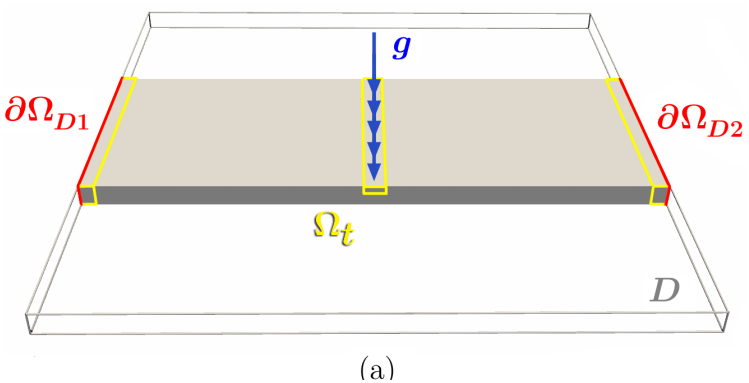

(a)

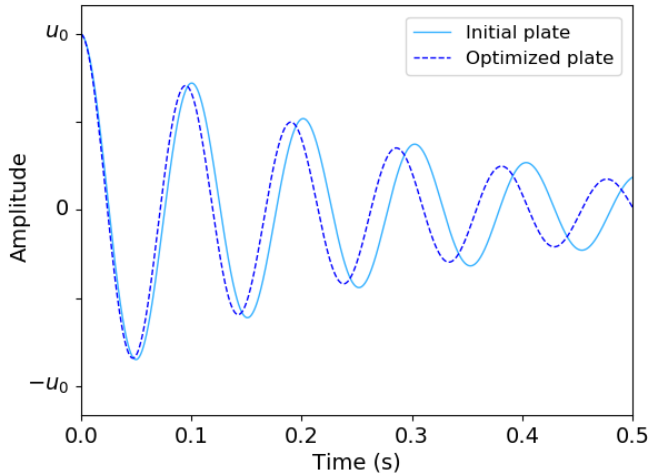

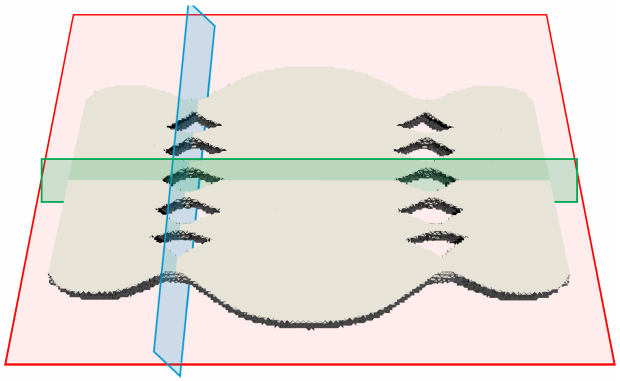

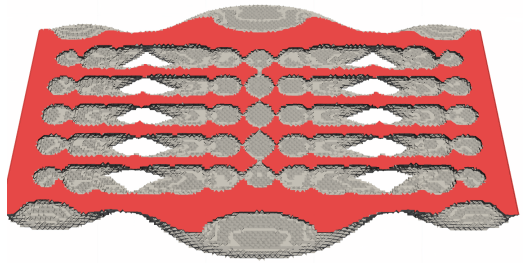

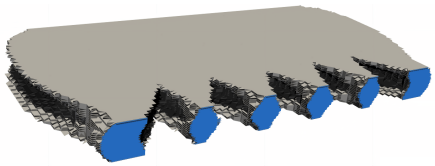

Running shoe

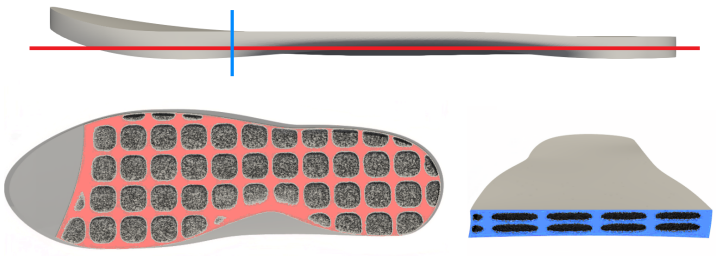

- HPC with `FreeFem++` and `OpenMPI`
- Unstructured mesh (Gmsh) with $\mathbb{P}_1$ tetrahedral elements
- Domain decomposition with `SCOTCH` or `METIS`
- 400 cores and sub-domains, 1 334 484 dof, about 15 hours
- Only one sequential operation: Advenction and redistancing of the level set function

Running shoe

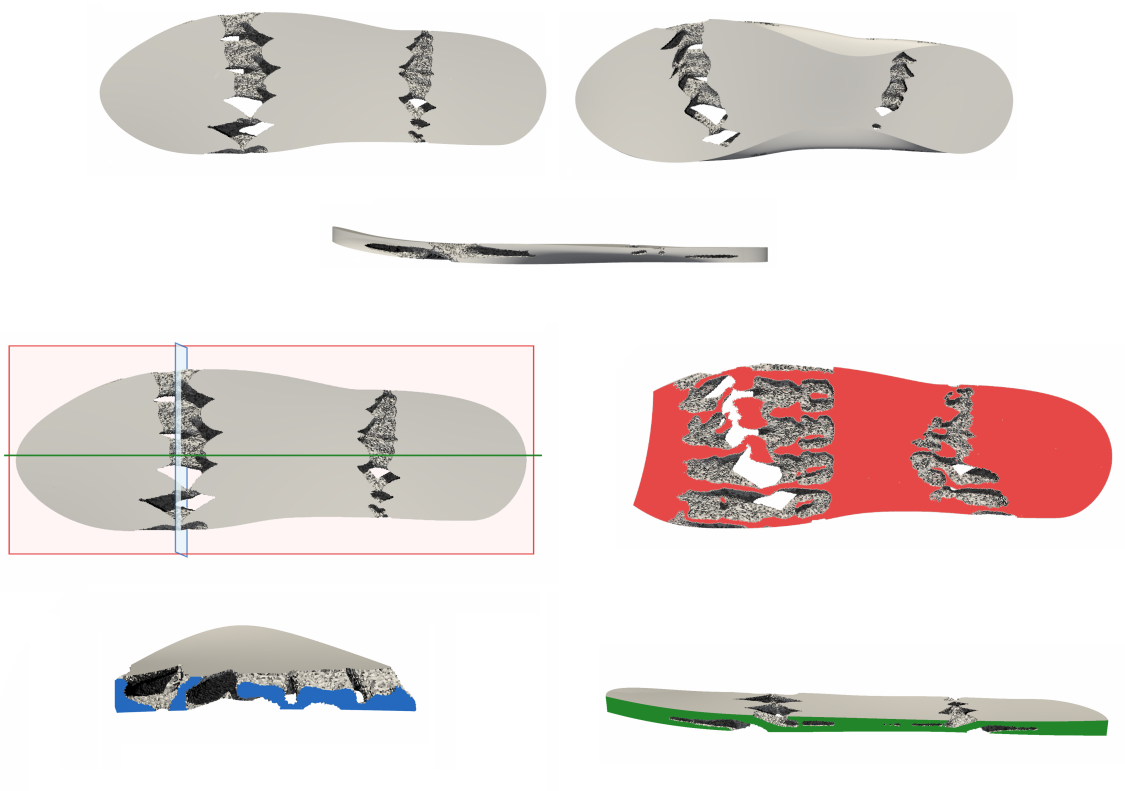

Compliance and volume evolution

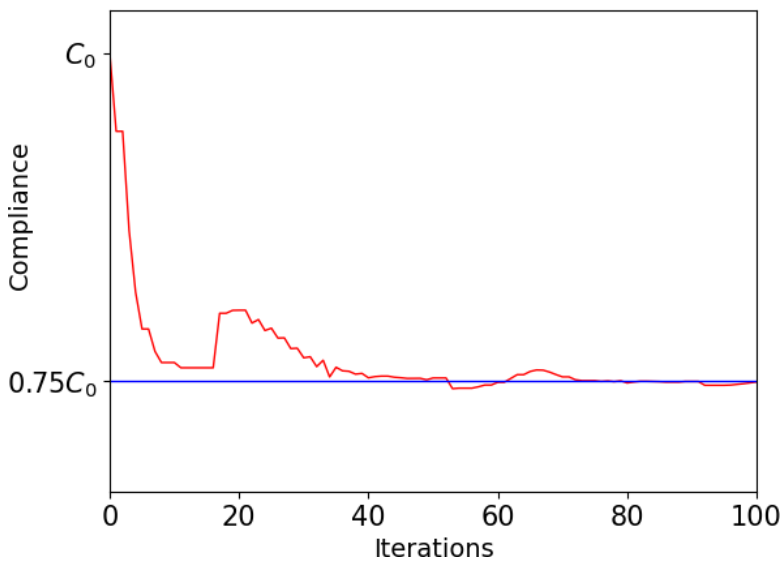

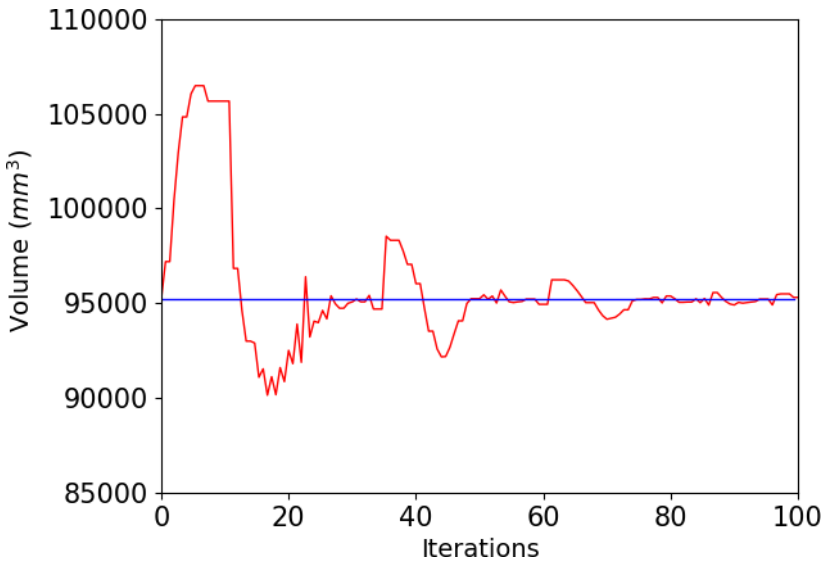

Free vibration when clamped at one or the other end

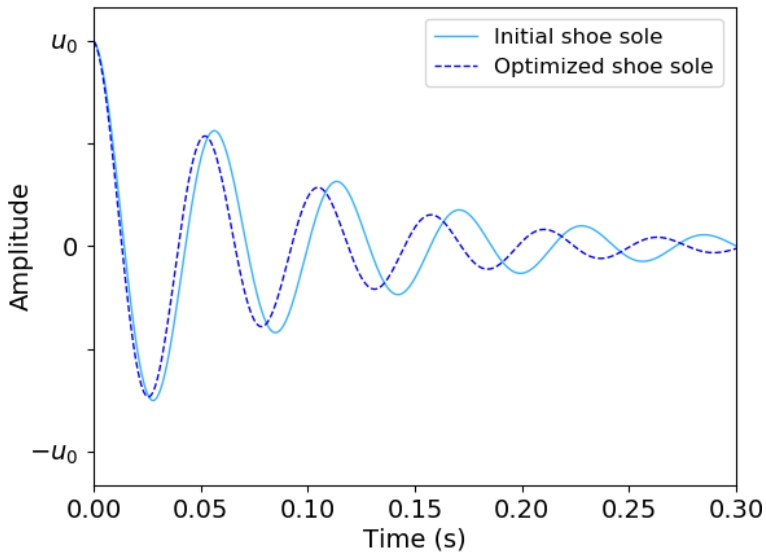

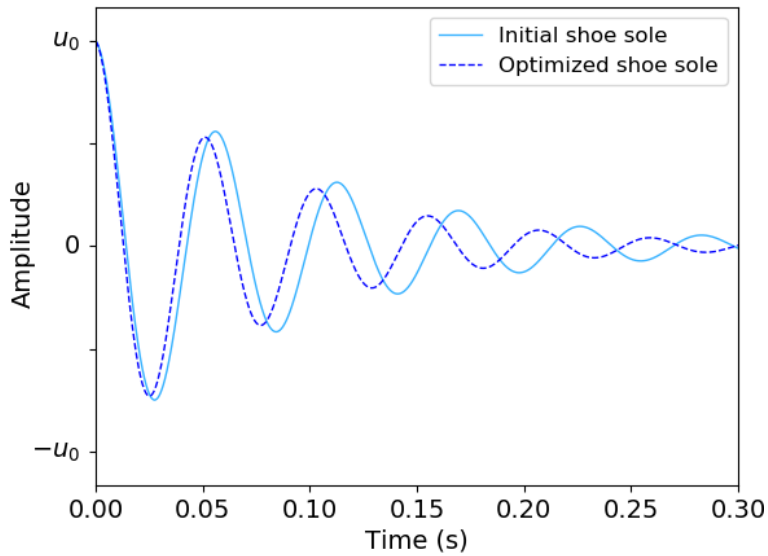

Conclusions

- Substantially improved damping properties of the optimized viscoelastic structures
- Impact of the material linear viscoelastic properties
- Local section shrinking due to the global criterion of compliance optimization for every 2D model
- 3D model creates inner microstructure designs
- Application to the shoe sole design within industrial constraints

Contributions

- A. Joubert, G. Allaire, S. Amstutz, J. Diani, 2023. Damping optimization of viscoelastic thin structures, application and analysis. Structural and Multidisciplinary Optimization, 66, 149.
- A. Joubert, G. Allaire, S. Amstutz, J. Diani, 2022. Damping otpimization of viscoelastic cantilever beams and plates under free vibration. Computers and Structures, 268, 106811.